Newtonian to non-Newtonian master flow curves of a bulk glass alloy Pd40Ni10Cu30P20

doi: 10.1063/1.122856

Newtonian to non-Newtonian master flow curves of a bulk glass alloy $Pd_{40}Ni_{10}Cu_{30}P_{20}$

Hidemi Kato,[a] Yoshihito Kawamura, and Akihisa Inoue
Institute for Materials Research, Tohoku University, Sendai, 980-8577, Japan

H. S. Chen
Bell Laboratories, Lucent Technologies, Murray Hill, New Jersey 07974

(Received 17 July 1998; accepted for publication 16 October 1998)

The viscosity and flow stress of a bulk $Pd_{40}Ni_{10}Cu_{30}P_{20}$ alloy glass near the glass transition were measured as a function of temperature and strain rate under compression. The steady-state viscosity of the glass for a given temperature remains constant at low strain rate, then decreases by many orders of magnitude above a critical strain rate. A master curve in term of the viscosity ratio η/η_N and the product $\eta_N\dot{\epsilon}$ has been constructed, where η and η_N are, respectively, the steady-state viscosity and Newtonian viscosity, and $\dot{\epsilon}$ is the strain rate. The flow stress also can be represented in terms of the product $\eta_N\dot{\epsilon}$. The master curves are fitted with a simple stress relaxation of the form $1-\exp[-t/\lambda]$ with $t=\dot{\epsilon}^{-1}$. © *1998 American Institute of Physics.* [S0003-6951(98)01651-9]

A number of alloy systems, such as Pd–Ni–P, Pd–Cu–Si, and Pt–Ni–P have been known for some time as very easy glass formers.[1] Recently Ln–Al–TM, Zr–Al–TM, Hf–Al–TM, and Mg–TM–Ln have been found to form a glass easily.[2] Here TM stands for transition metals Fe, Co, Ni, and Cu. These alloys can be cast into a bulk glass from a melt at cooling rates as low as 10 K/s, and the glasses show a wide supercooled liquid region before crystallization. The high stability and fluidity of these glass alloys opens the possibility of forming bulk materials of various shapes, at elevated temperatures, with straightforward processes, such as casting, forging, extrusion, and consolidation. Flow and deformation of alloy glasses at elevated temperature near a glass transition, T_g, have been reported.[3] The Newtonian viscosity, η_N, of alloy glasses has a temperature dependence following a Vogel–Fulcher–Tammann (VFT) expression,[4–6] $\eta_N=\eta_0\exp[Q/(T-T_0)]$, where T_0 is the VFT temperature. At temperatures below T_g, alloy glasses deform inhomogeneously and the fracture strength depends on the strain rate but remains nearly constant with varying temperatures.[3,7]

In this letter, we report on the viscosity of a $Pd_{40}Ni_{10}Cu_{30}P_{20}$[8] alloy glass near the glass transition, ($T_g=575$ K), as a function of temperature and strain rate with compression test. The steady-state viscosity of the glass at a given temperature remains constant at low strain rate, $\dot{\epsilon}$, then decreases above a critical strain rate, $\dot{\epsilon}_c$, indicating Newtonian to non-Newtonian flow, and the viscosity (η) decreases by many orders of magnitude. The critical strain rate, $\dot{\epsilon}_c$, strongly depends on temperature, and inversely scales to Newtonian viscosity (η_N). We construct a master curve for a glass alloy in terms of the viscosity ratio (η/η_N) and the product ($\eta_N\dot{\epsilon}$) of the viscosity (η_N) and strain rate ($\dot{\epsilon}$). The flow stress, σ_f, also can be represented by a master curve in terms of the product $\eta_N\dot{\epsilon}$. The flow stress, σ_f, increases proportionally with strain rate in the Newtonian regime and tends to flatten out at a high strain rate in the non-Newtonian regime. A relaxation model is proposed and the master curves are fitted with a simple stress relaxation function of the form $1-\exp[-1/t_1\dot{\gamma}]$ where t_1 is a time constant and $\dot{\gamma}$ is the shear rate.

Alloy ingots were prepared by arc melting pure metals in a purified argon atmosphere. Cylindrical samples of a $Pd_{40}Ni_{10}Cu_{30}P_{20}$ alloy glass 2 mm in diameter were obtained by melt casting into a Cu mold. Glassy structure of the cast samples was confirmed by x-ray diffraction. Thermal properties were measured by differential scanning calorimetry (DSC). The onset of the glass transition temperature T_g and the onset of crystallization were determined at 0.33 K/s to be 575 and 655 K, respectively. For a compressive mechanical test, cylindrical samples, 2 mm diameter×4 mm length, were cut from the cast glass alloy and the surfaces polished parallel. The compression tests were conducted using an Instron-type.

Figure 1 shows the strain-rate dependence of the stress–strain curves at $T=573$ K. At low strain rate $\dot{\epsilon}<1.0\times10^{-3}$/s, the stress σ increases monotonically with strain ϵ and attains a steady-state flow stress σ_f. At high strain rate,

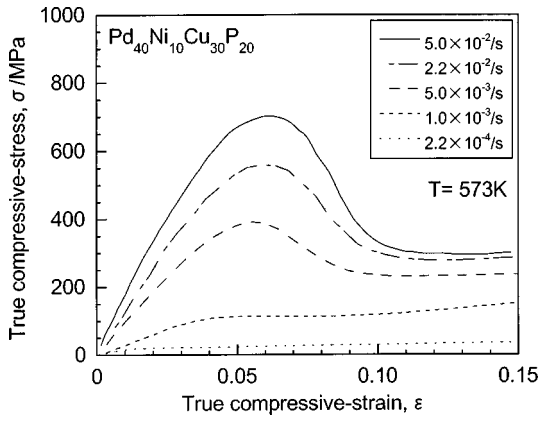

FIG. 1. Stress–strain curves at various strain rates $\dot{\epsilon}$. The example is given tested at $T=573$ K.

[a]Electronic mail: hikato@imr.tohoku.ac.jp

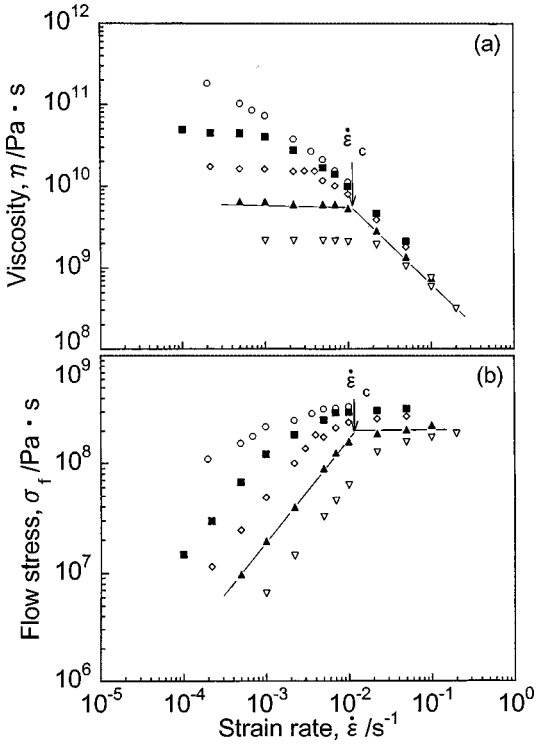

FIG. 2. The strain rate $\dot{\epsilon}$ dependence of viscosity η (a), and flow stress σ_f (b) at various temperatures: 568 K (○), 573 K (■), 578 K (◇), 583 K (▲), and 588 K (▽). The term $\dot{\epsilon}_c$ is the critical strain at the intersection of two viscosity lines.

$\dot{\epsilon} > 5\times10^{-3}$/s, σ increases initially attaining a maximum value at strain $\epsilon \sim 6\times10^{-2}$. It then decreases and attains a steady-state value for $\epsilon > 10\times10^{-2}$. Such a stress overshoot phenomenon has been observed previously in Zr-based glass alloys.[3] The steady-state viscosity $\eta(=\sigma_f/3\dot{\epsilon})$ was thus obtained.

The strain rate dependence of viscosity η and flow stress σ_f are illustrated in Figs. 2(a) and 2(b), respectively. As shown in Fig. 2(a), η remains constant for $\dot{\epsilon} < \dot{\epsilon}_c$ and then decreases drastically for $\dot{\epsilon} > \dot{\epsilon}_c$. At much higher $\dot{\epsilon}$, log η vs log $\dot{\epsilon}$ curves show a slope of -1. We define here the critical strain rate $\dot{\epsilon}_c$ at the intersection of viscosity $\eta(\dot{\epsilon})$ lines in the low and high $\dot{\epsilon}$ regime. The term $\dot{\epsilon}_c$ is also the critical strain rate, above which the strain–stress curves show a stress overshoot (Fig. 1). The Newtonian viscosity η_N decreases by two orders of magnitude from $\sim 3\times10^{11}$ Pa s at 568 K to 2×10^{9} Pa s at 588 K, and the critical strain rate $\dot{\epsilon}_c$ appears vary nearly inversely proportional to η_N, from 2×10^{-4} s^{-1} to 3×10^{-2} s^{-1}. The corresponding strain-rate dependence of flow stress $\sigma_f(=\sqrt{3}\dot{\epsilon}\eta)$ is shown in Fig. 2(b). The flow stress σ_f increases linearly with $\dot{\epsilon}$ initially then deviates from the linearity and attains a plateau at $\dot{\epsilon} > \dot{\epsilon}_c$. It may be noted that for the temperature range studied at very high strain rate, e.g., $\dot{\epsilon} > 5\times10^{-2}$ s^{-1}, the viscosities and flow stresses tend to merge together and vary slightly with temperature in contrast with the large change in the Newtonian viscosity η_N. The limiting maximum flow stress σ_f^* decreases slightly with increasing temperature from 3.8×10^{8} Pa s at $T=568$ K to 2.1×10^{8} Pa at $T=588$ K.

The normalized viscosity η/η_N and the flow stress σ_f plotted against the product ($\eta_N\dot{\epsilon}$) of strain rate and Newtonian viscosity are shown in Figs. 3(a) and 3(b), respectively.

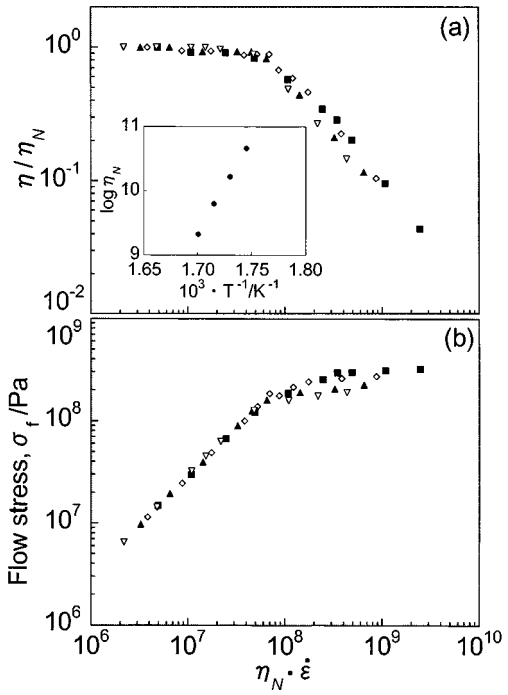

FIG. 3. The normalized viscosity η/η_N (a), and the flow stress σ_f (b) vs $\eta_N\dot{\epsilon}$, the products of Newtonian viscosity and strain rate $\dot{\epsilon}$ at various temperatures: 573 K (■), 578 K (◇), 583 K (▲), and 588 K (▽). The temperature dependence of η_N is shown in the inset.

The temperature dependence of the viscosity, η_N, is shown in the inset. The viscosity $\eta_N = \eta_0 \exp\,[Q/kT]$ with $\eta_0 = 3.75\times10^{-48}$ Pa s and $Q \sim 5$ eV. As shown in Figs. 3(a) and 3(b), η/η_N and σ_f, in the non-Newtonian regime, i.e., $\eta_N\dot{\epsilon} > 10^8$ Pa, decrease with increasing temperature. By horizontal shift the log(η/η_N) vs log($\eta_N\dot{\epsilon}$) curves to $T=578$ K, a master curve is obtained as shown in Fig. 4(a).

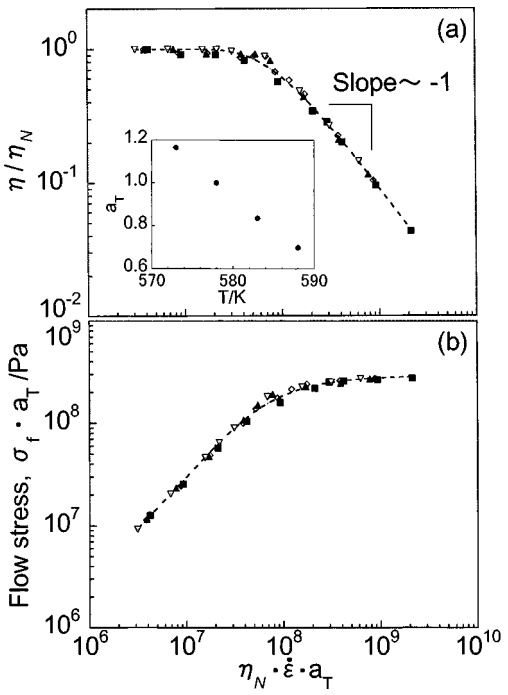

FIG. 4. A master curve of viscosity η/η_N (a) and flow stress σ_f (b) in terms of the product $\eta_N\dot{\epsilon}$ at $T=578$ K. Shift factors a_T are shown in the inset. The curves are fitted with a relaxation function of the form $1-\exp(-1/t_1\dot{\epsilon})$, with the time constant, $t_1=180$ s.

The shift factors a_T are shown in the inset. As stated previously, at high $\eta_N\dot{\epsilon}$, the log η/η_N vs log $\eta_N\dot{\epsilon}a_T$ curve shows a slope of -1. Using the same shift factors, we are able to obtain a master curve in terms of $\sigma_f \cdot a_T$ and $\eta_N\dot{\epsilon}\cdot a_T$ shown in Fig. 4(b). Since $\log(\sigma_f \cdot a_T)=\log(\eta\dot{\epsilon}\cdot a_T)$ $=\log(\eta/\eta_N)+\log(\eta_N\dot{\epsilon}\cdot a_T)$, in fact, the shape of $\log(\eta/\eta_N)$ vs $\log(\eta_N\dot{\epsilon}\cdot a_T)$ and the $\log(\sigma_f \cdot a_T)$ vs $\log(\eta_N\dot{\epsilon}\cdot a_T)$ master curve is identical upon rotating each other by 45°.

Non-Newtonian flow in a polymer system has been extensively investigated theoretically and experimentally.[9] Theories in general treat viscosity of melt polymers caused by entanglements which decrease with shear rates. At high shear rates, the time required to form an entanglement is longer than the transit time of a group of segments over a potential entanglement site. As a result, entanglements do not have time to form and viscosity decreases. The initial structure is broken down and the new steady-state structure has the entanglement formation time comparable to the transit time. It is the reconfiguration of entanglements that causes the non-Newtonian flow. The theories predict that the non-Newtonian viscosity, at very high strain rates, follows power law, i.e., $\eta\sim\dot{\gamma}^{-n}$ with $n=6/7$[10] and 3/4.[11] Here $\dot{\gamma}$ is a shear rate. Recent computer simulations in Lennard-Jones glasses[12] reveal that the shearing action changes the liquid structure so that there is a tendency to reorganize the liquid directionally, facilitating flow and reducing viscosity, and the steady-state viscosity approaches asymptotically a maximum (τ^*) at very high shear rate. In the non-Newtonian flow regime at constant shear rates $\dot{\gamma}>\tau^*/G_\infty\lambda$, there exists an overshoot in the stress versus strain curve because the structural breakdown processes are much slower than the shear relaxation processes governing the viscosity, (where G_∞ is a shear rigidity modulus and λ is shear relaxation time). It seems clear that the observed nonlinear and non-Newtonian behaviors are fundamental properties of a liquid or glassy state. Accordingly we propose the relaxation model to illustrate the flow behavior of alloy glasses as follows.

When a viscoelastic material is deformed at a constant shear rate $\dot{\gamma}$, at first the stress rises linearly with time, $\tau(t)$ $=G_\infty\cdot\dot{\gamma}t=G_\infty\gamma(t)$, as a liquid takes time to respond structurally. Since a liquid will not support a static stress, it flows and the rate of increase of the stress decreases. It attains a limiting steady-state value, $\tau_s=G_\infty\lambda\dot{\gamma}=\eta\dot{\gamma}$, where λ is a shear relaxation time. In theory then, the strain rate is increased without limit, and τ_s will also become higher without limit. However, the stress will reach a critical level, τ_c, at which a substantial structural breakdown takes place. For example, the initial cooperative domains may break down, or the shear reorganizes the liquid directionally to facilitate the flow. The new structure has a shorter relaxation time $\lambda'<\lambda$, $\tau_c=G_\infty\lambda'\dot{\gamma}$ and, $\eta=\tau_c/\dot{\gamma}=G_\infty\lambda'<\eta_N$. Appreciable decreases in viscosity, i.e., non-Newtonian flow, will be observed. Ideally the structure of the liquid changes through relaxation even at low strain rate and low flow stress. It is at a critical stress τ_c that an appreciable deviation in η from the Newtonian flow is observable. With a further increase in strain rate, structure changes further and the viscosity η and the shear relaxation time λ' decreases accordingly while the flow stress τ may increase slightly. The steady-state stress asymptotically approaches a maximum at very high shear rate. The limiting stress (τ^*) may be interpreted as the actual cohesive strength of the materials, The maximum elastic shear strain $\gamma_e^*=\tau^*/G_\infty$, which the liquid can support, is thus a characteristic of materials and may depend slightly on atomic configuration of the liquid. The maximum flow strength, τ^* in general, is several times smaller than the ultimate fracture strength of the solid glass τ_u, the fracture strength of a glass when $\dot{\gamma}\gg\lambda^{-1}$.

We arrive at two end conditions for the flow stress

$$\tau_s=G_\infty\lambda\dot{\gamma}=\eta_N\dot{\gamma} \quad \text{for} \quad \dot{\gamma}<\tau_c/G_\infty\lambda<\tau^*/G_\infty\lambda, \tag{1a}$$

$$\tau_s=\tau^*=G_\infty\dot{\gamma}_e^* \quad \text{for} \quad \dot{\gamma}>\tau^*/G_\infty\lambda. \tag{1b}$$

The conditions set forth above can be approximated by, considering the relaxation mechanism for the non-Newtonian flow proposed above, a simple stress relaxation function

$$\tau_s=\tau^*t_1\dot{\gamma}[1-\exp(-1/t_1\dot{\gamma})] \tag{2a}$$

and

$$\eta/\eta_N=[1-\exp(-1/t_1\dot{\gamma})], \tag{2b}$$

where $t_1=G\lambda/\tau^*=\lambda/\gamma_e^*$. We found the Young's modulus of the Pd-based glass, $E_\infty\sim5\times10^{10}$ Pa and estimated the maximum elastic strain of the liquid $\gamma_e^*\sim\tau^*/G_\infty$ $\sim\sqrt{3\sigma^*/E_\infty}=10^{-2}$. The experimental data are fitted with Eqs. (2a) and (2b) and shown in Fig. 4. In the fitting, we adopt compressive stress σ_f and compressive strain rate $\dot{\epsilon}$, in place of τ and $\dot{\gamma}$ in Eqs. (2a) and (2b). It simply effects upon the time constant t_1 accordingly. The agreements are very satisfactory.

It is extraordinary that experimental viscosities of a glass alloy $Pd_{40}Ni_{10}Cu_{30}P_{20}$ can be fitted well with simple stress relaxation of the form $G(t)=G_\infty[1-\exp(-t/\lambda)]$ of a single relaxation time λ. It predicts that the viscosity of the alloy glass follows the power law $\eta\propto\dot{\epsilon}^{-n}$ at very large strain rates as have been established in polymers.[9] We also note that the maximum elastic shear strain γ_e^*, which liquid can sustain, is small in 10^{-2} for the alloy glass as compared with γ_e^* $=10^{-1}$ for polymer glass. Further investigations on flow properties for other alloy glasses are of great interest.

[1] H. S. Chen, Rep. Prog. Phys. **43**, 353 (1980).
[2] A. Inoue, T. Zhang, and T. Masumoto, Mater. Trans., JIM **11**, 1005 (1991).
[3] Y. Kawamura, T. Shibata, A. Inoue, and T. Masumoto, Appl. Phys. Lett. **69**, 1208 (1996).
[4] H. S. Chen and D. Turnbull, J. Chem. Phys. **48**, 2560 (1968).
[5] H. S. Chen and M. Goldstein, J. Appl. Phys. **43**, 1642 (1972).
[6] E. Bakke, R. Busch, and W. L. Johnson, Appl. Phys. Lett. **67**, 3260 (1995).
[7] Y. Kawamura, H. Kato, A. Inoue, and T. Masumoto, Appl. Phys. Lett. **67**, 2008 (1995).
[8] A. Inoue, N. Nishiyama, and T. Matsuda, Mater. Trans., JIM **37**, 181 (1996).
[9] J. D. Ferry, *Viscoelastic Properties of Polymers* (Wiley, New York, 1970).
[10] F. Bueche, *Physical Properties of Polymers* (Interscience, New York, 1962).
[11] W. W. Graessley, J. Chem. Phys. **47**, 1942 (1967).
[12] D. M. Heyes, J. J. Kim, C. J. Montrose, and A. Litovitz, J. Chem. Phys. **73**, 15 (1980).